JOURNAL OF MATERIALS SCIENCE 19 (1984) 3049–3058

Linear shaped-charge (LSC) collapse model

GEORGE A. HAYES
Materials Engineering Branch, Naval Weapons Center, China Lake, California 93555, USA

A model is presented describing the sequence of events leading up to linear shaped-charge (LSC) liner collapse and jet/slug formation. Metallographic techniques were utilized to determine the relative efficiency of various liner configurations, i.e. the volume percentage of metal participating in jet formation. The microstructures of selected LSC fragments and some of the more interesting structural details and their implications are discussed. Timing screens and flash X-ray techniques were employed to provide data concerning the velocity of LSC jet and slug fragments and their relationship to liner configuration and material properties.

1. Introduction

Although linear shaped-charges (LSCs) have been utilized for many years by both industry and the military, the manner in which they operate, e.g. the collapse process, is not completely understood. In this paper a model is presented describing the sequence of events leading up to LSC liner collapse and jet/slug formation. A metallographic technique was utilized to reconstruct the LSC collapse process and to determine the efficiency of various liner configurations, i.e. the volume percentage of liner participating in jet formation. From the microstructure of recovered elements of collapsed charge liners, much can be learned about the deformation processes that have occurred.

2. Experimental methods

A schematic drawing of a typical LSC is shown in Fig. 1. The liner material, usually a metal, is collapsed by the shock front of the detonating explosive. The explosive is initiated at the forward end of the liner. Two grades of steel liner material were utilized in this study – AISI 1020 and AISI 1008. Composition B was used as the explosive charge. The outer surface of selected charge liners was electroplated with a 25 to 50 μm thickness of silver to facilitate in fragment identification and to aid in defining the deformation mode.

After detonation, the velocities of various LSC fragments were measured using ballistic timing screen techniques and pulse flash radiography. Shaped-charge fragments were captured after detonation by either statistically test firing into a controlled-density recovery material or firing vertically into air and recovering the fragments. Firing into air allowed the LSC collapse process to go to completion, whereas firing into the controlled-density recovery system terminated the collapse process upon impact. The advantage of

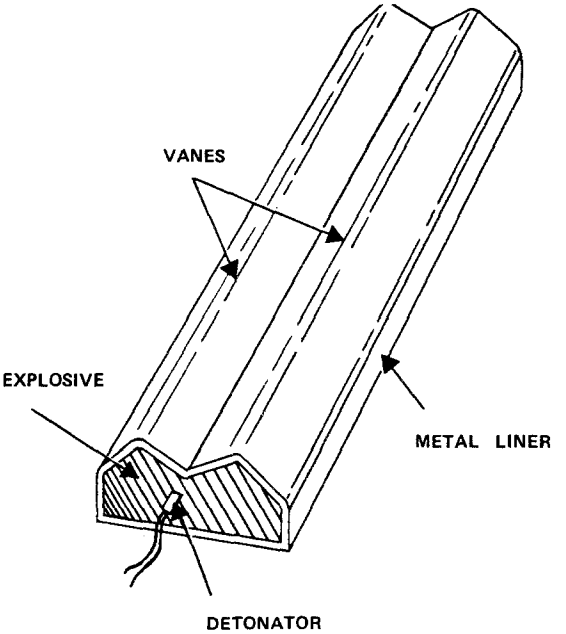

Figure 1 Schematic diagram of typical linear shaped-charge.

0022–2461/84 $03.00 + .12

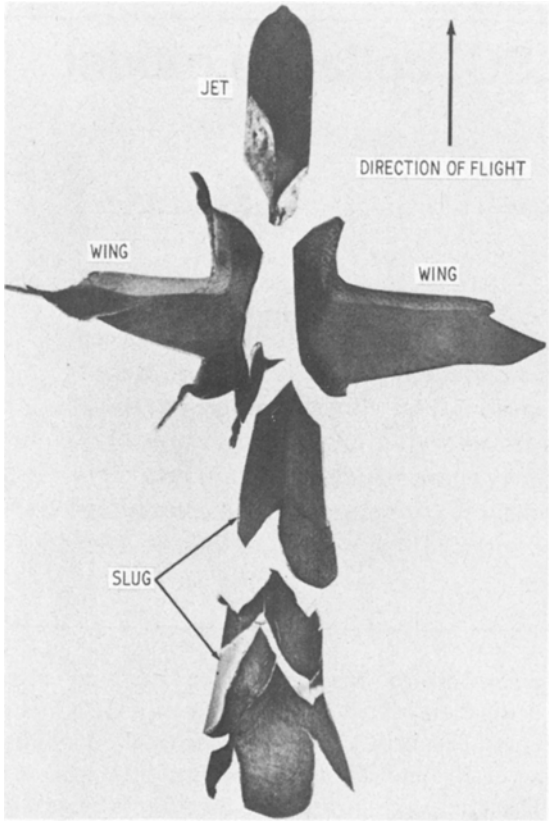

Figure 2 Mock-up of flight pattern assumed by fragments in Test 1.

using controlled-density recovery is that by varying stand-off distance, ejecta fragments produced after various stages of liner collapse can be recovered.

After recovery, each fragment was sectioned, polished, and etched. By matching the shape and microstructure of the recovered fragments it was possible to postulate a model of the LSC collapse process. The microstructural analysis of the fragments illustrated the metal flow-line geometry, indicating how each fragment was formed, and made it possible to calculate the efficiency of various liner configurations.

3. Results and discussion

3.1. Metallography

The techniques described above were used to investigate various LSC configurations and test arrangements. The results of the first test are used to illustrate the general way LSC fragments are formed, and to construct their probable configuration during flight. The second test series was used to depict the detailed microstructure of each basic type of LSC fragment, illustrating the characteristics of metal flow and fragment formation. The final test series was conducted to aid in reconstructing the LSC collapse process.

3.1.1. Test 1

In the first test the liner material was a normalized AISI 1020 steel 0.64 cm thick with an included angle of 110°. After firing into air the fragments were recovered and found to be rod-like in shape. Each rod was transversely cross-sectioned, polished, and etched. By fitting together the resulting fragment shapes and matching their microstructural flow lines, the pieces were arranged into what is considered to be the flight pattern assumed by the fragments before impact. A mock-up of this pattern is shown in Fig. 2. For identification purposes the fragments in the shape of a wing are termed "jet wings". As will be seen later, the wings are the remains of the LSC vanes that did not participate in either jet or slug formation. The elements in front of the wings are referred to as the "jet", while those behind the wings are collectively designated the "slug". The detailed structure of a typical jet, jet wing and slug fragment will be considered in the next test series.

3.1.2. Test 2

This test investigates LSC fragment formation from a more ductile liner material. An annealed AISI 1008 steel 0.472 cm thick was utilized. The liner had an included angle of 120°. The outer surface of the liner was plated with a thin layer of silver. Fig. 3a illustrates the cross-sectional profile and microstructure of the charge liner prior to firing. The shaped-charge was detonated into air, and the fragments were recovered and prepared for metallographic examination. Fig. 3b is a mock-up what is considered to be the probable flight pattern of the LSC fragments.

Several differences in fragment size and distribution from that of the preceding test are apparent. First, there is relatively less material left in the jet wings. Second, there are fewer fragments, i.e. they did not break up as much. Third, the main jet and slug elements are much larger than for the preceding test. All these differences are related to the liner composition and heat treatment, which for this test would lead to a more ductile, fracture-resistant material. The microstructure and plastic flow experienced by each LSC element will now be described.

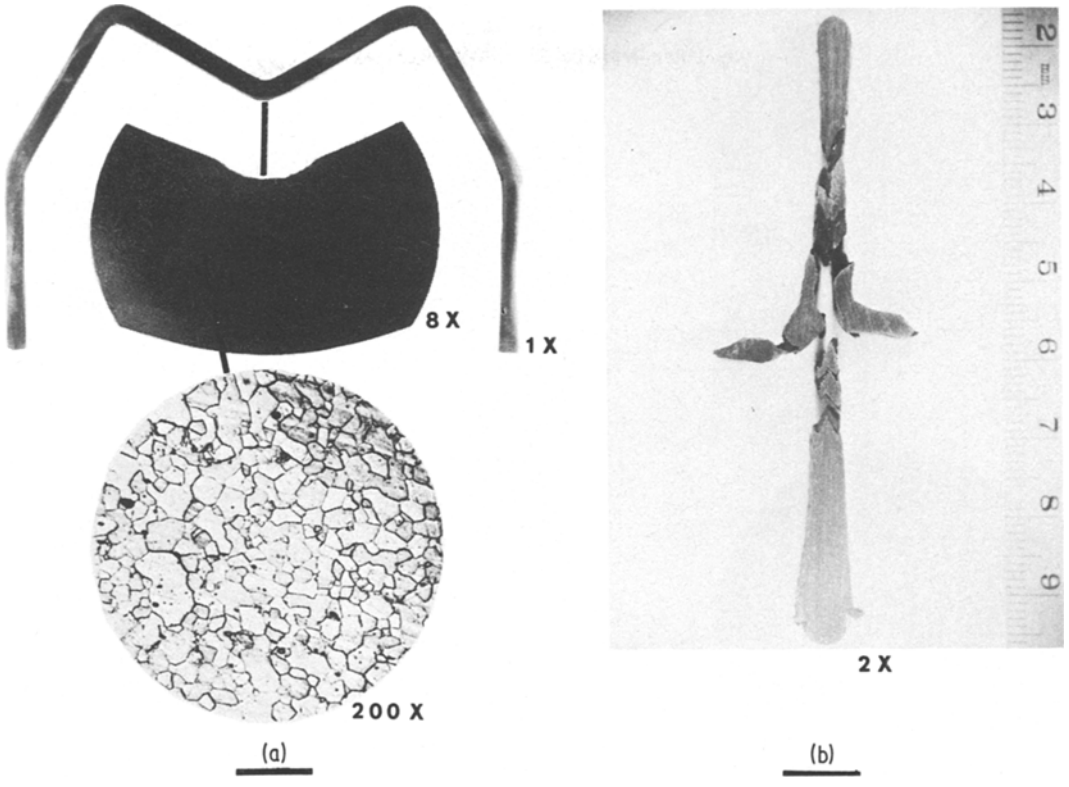

Figure 3 (a) Cross-section and microstructure of liner used in Test 2. (b) Mock-up of flight profile assumed by fragments.

Fig. 4 shows a cross-section of the LSC jet formed by the detonating explosive. The metal flow patterns are illustrated in the photomicrographs accompanying the jet cross-section. Observe that the grain structure changes continuously from the surface of the jet inward toward its centre. The silver plating over the surface of the jet should be noted. It is apparent that the jet was formed as a result of inward and forward flow of the metal from near the outer (silver plated) surface of the liner, leaving the silver coating and grains near the surface relatively undisturbed. Apparently little micro-deformation took place in the metal located near the surface of the jet. The central core of the jet, however, experienced considerable deformation and heat, and is completely recrystallized. In the region where the jet fractured (by shear) from the jet follower, complete recrystallization and varying amounts of grain growth occurred, implying that a large temperature rise took place in this region. The increase in temperature was caused by the extreme deformation incurred during collapse of the liner. The time required for this deformation more than likely did not exceed 1 msec. Once heated, the fragments probably stayed hot for a few seconds (until they were caught). If one estimates [1] the temperature increase required to cause the observed grain growth, assuming a growth time of a few seconds, then it appears that the region of the jet where the grains grew the most, experienced an average temperature rise of at least 900° C.

Fig. 5 shows a cross-section of one of the two jet wings and its related microstructure. The original explosive–liner interface was at the bottom of what is now the wing. The dark band near the outer (silver plated) surface of the wing should be noted. Little plastic deformation took place in the band, whereas the rest of the wing experienced quite severe micro-deformation. The abrupt change in structure was caused by shock-wave interactions [2]. The explosive shock wave was reflected at the free surface as a release wave. The interaction of this wave and the remaining incident compressional wave resulted in the well-defined boundary separating the shock-twinned structure from the unshocked material. The metal near the left surface of the jet wing is recrystallized,

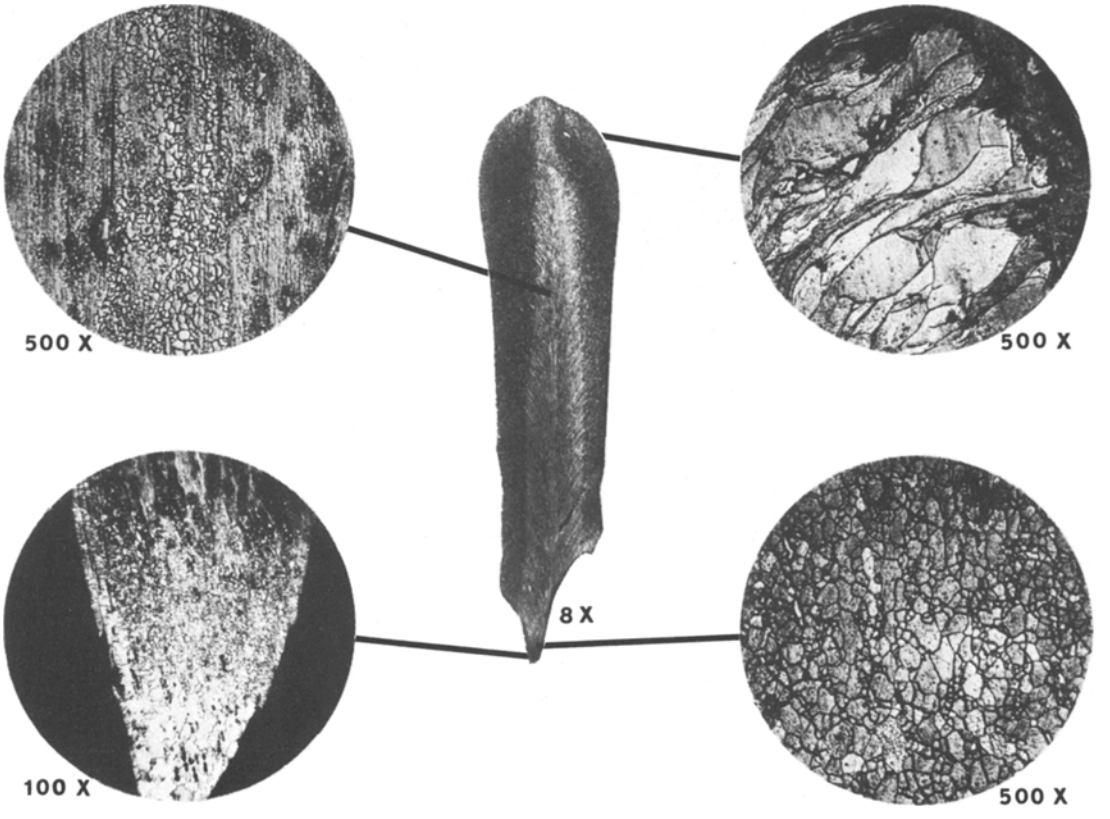

Figure 4 (a) Microstructure and (b) cross-section of jet formed in Test 2.

similar to the structure at the central core of the jet. Apparently the jet (and the slug as will be shown later) is formed by the material in the vanes of the liner flowing inward, caused by the focused action of the explosive shock wave. This action terminates before all of the vane material is utilized, leaving the jet wings. Notice the flow lines turning forward (toward the jet) and backward (toward the slug) at the left side of the wing.

The cross-section of the slug and some microstructural details are shown in Fig. 6. Macroscopic shear is evident in a region extending from the forward end to near the base of the slug. Two families of shear trajectories exist in this region. Note that isolated positions near the surface of the slug underwent recrystallization and grain growth. Time, temperature and plastic deformation are necessary for recrystallization to occur. In these experiments the time available for transport processes was relatively short. Apparently the heat generated during the collapse of the liner provided the driving force to cause nucleation of isolated grains in regions that underwent a critical amount of strain (probably less than 5%). In contrast, the much greater strain experienced in the core of the slug brought about general recrystallization in this region. It is estimated [3] that during formation of the slug it reached a temperature of about 750° C.

3.1.3. Test 3

The third test involved a smaller-scale charge liner than those previously described. The liner material was an annealed AISI 1008 steel 0.183 cm thick with an included angle of 120°. In this test the LSC was fired into a recovery tank containing a viscous fluid (cellulose solution). The horizontal axis of the liner was placed at an angle with respect to the recovery tank such that the liner-to-fluid distance varied. In this way it was possible to interrupt the liner collapse process after various degrees of completion. Details describing this technique are discussed elsewhere [4]. After detonation, the fragments were recovered from the tank. The overall cross-sectional shape of the

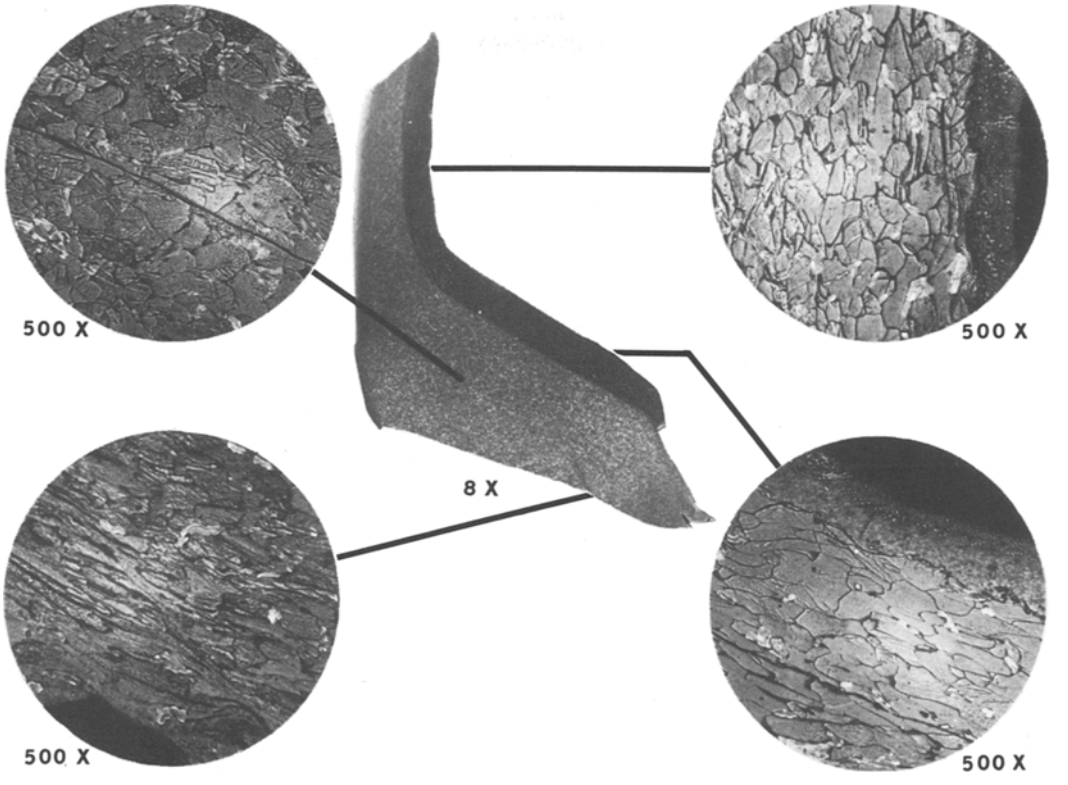

Figure 5 Cross-section and some microstructural details of jet wing formed in Test 2.

fragments varied from position to position along the length of the original liner. Cross-sections were taken at appropriate positions perpendicular to the liner axis. These cross-sections were polished and etched for metallurgical examination.

Fig. 7 illustrates the macrostructure of the LSC and its fragments. The figure represents various stages in the liner collapse process. Fig. 7a shows the structure of the liner near its apex before detonation of the explosive charge.

Fig. 7b illustrates the liner after the collapse process has started. Note the clearly recognizable slug that is beginning to form at the bottom (apex) of the liner. The liner has transformed into what was earlier in this paper termed jet wings. In Fig. 7c more of the jet wing has flowed into the centre, enlarging the slug, decreasing the size of the wing, and starting a forward jetting action. The final slug and jet that was formed from the liner are shown in Figs. 7d and e, respectively.

It should be remembered that the series of pictures shown in Fig. 7 probably does not exactly represent the collapse process that would be encountered in air since the fluid used to inhibit the collapse probably caused some change in the deformation process. However, the general trend is probably also valid in air.

Fig. 8 shows the cross-section and microstructure of the fully formed jet from this test series. In general, even though the size has been considerably reduced, the structure of the jet is quite similar to that of the other larger jets that have been studied. One quite important structural detail should be noted: the large shock-twinned grains near the surface of the jet (indicated by the arrow). These grains were twinned during exposure to the shock wave during the detonation process (before metal transport had a chance to take place). However, the twins (and the surface grains) have not been noticeably deformed, even though the jet as a whole has undergone extreme macroscopic plastic deformation. It is evident that the liner surface material flowed forward into the jet with very little microscopic shear deformation taking place. In the internal part of the jet, however, quite complex deformation mechanisms were in play, causing a highly deformed recrystallized microstructure.

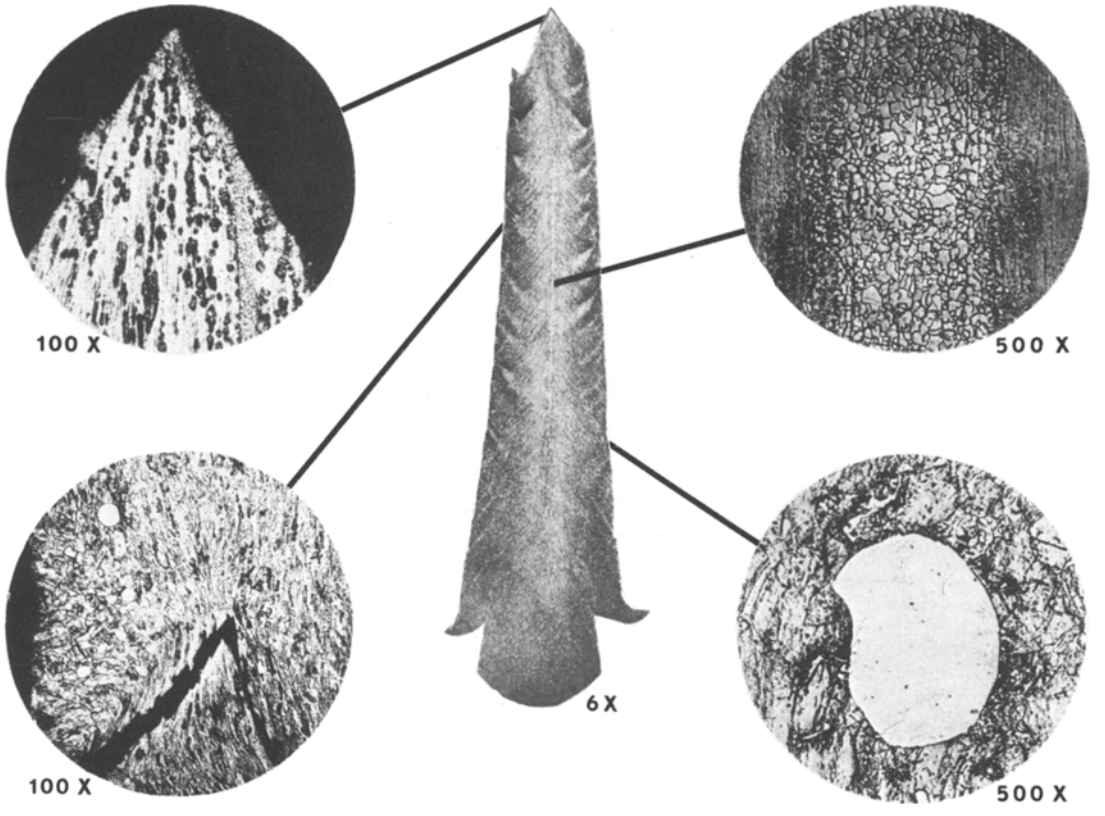

Figure 6 Cross-section and microstructure of slug formed in Test 2.

3.2. Efficiency of charge liners

The geometry of LSC liners allows the determination of the relative efficiency of each liner configuration, i.e. the volume percentage of metal participating in jet formation. This is possible because during manufacture the liners are bent from flat stock into the desired geometry, and the total volume of material available in the vanes for participation in the collapse process is known. By recovering, sectioning and measuring the cross-sectional area of the rod-like fragments, the relative volume of metal in each type of fragment may be calculated.

An example of such an analysis for some representative liner configurations is shown in Table I, which correlates shaped-charge liner material and geometry with the type, number, and relative volume of fragments formed. It is seen that of the liner configurations investigated, the most efficient is composed of the more ductile 1008 steel and has an apex angle of 120°.

3.3. LSC jet/slug velocity

The velocity of jet and slug fragments from various liner configurations is summarized in Table II. Velocities were determined by pulsed flash radiography and by means of ballistic timing screen techniques. A typical distance–time plot for a jet leading element is shown in Fig. 9. Velocity was measured by calculating the initial slope of the distance–time curve. The data in Table II indicate that increased liner efficiency (higher percentage of material flowing into the jet) leads to higher jet velocity while increased slug mass yields slightly lower slug velocity. This is illustrated by the plot of fragment weight distribution (%) against velocity, shown in Fig. 10.

4. Linear shaped-charge collapse model

Correlation of the results collected from several test firings has tended to give an insight into the LSC collapse process, and has aided in defining the deformation mechanism involved in jet and slug formation. In particular, Test 3 is most helpful in illustrating the shaped-charge liner collapse mechanism. Fig. 11 shows another cross-section of the partially collapsed shaped-charge liner recovered from this test. This cross-section illus-

TABLE I Correlation of LSC parameters with fragment distribution

Material	Thickness (cm)	Apex angle (deg)	Distribution of metal (%)			Number of jet fragments	Number of slug fragments
			Jet	Wings	Slug		
1020 steel	0.64	110	18.2	38.1	43.7	1	1
1020 steel	0.64	120	21.3	37.9	40.8	3	3
1020 steel	0.64	135	15.5	68.2	16.3	1	1
1008 steel	0.47	120	28.6	25.5	45.9	2	2
1008 steel	0.18	120	29.4	33.8	36.8	2	1

TABLE II Correlation of LSC parameters with jet/slug velocities

Material	Thickness (cm)	Apex angle (deg)	Jet velocity ($m\ sec^{-1}$)	Slug velocity ($m\ sec^{-1}$)
1020 steel	0.64	110	3000	1400
1020 steel	0.64	120	3150	1450
1020 steel	0.64	135	2800	1550
1008 steel	0.47	120	3250	1450
1008 steel	0.18	120	3050	1400

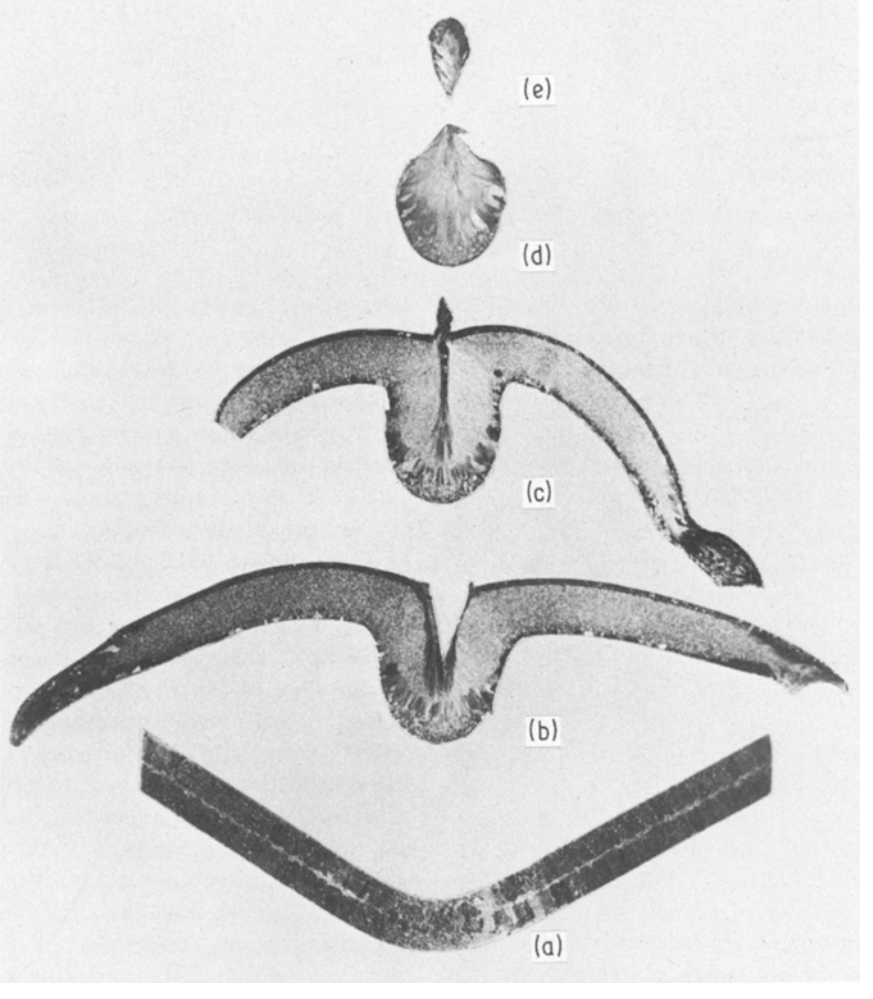

Figure 7 Macrostructure of LSC showing various stages of liner collapse.

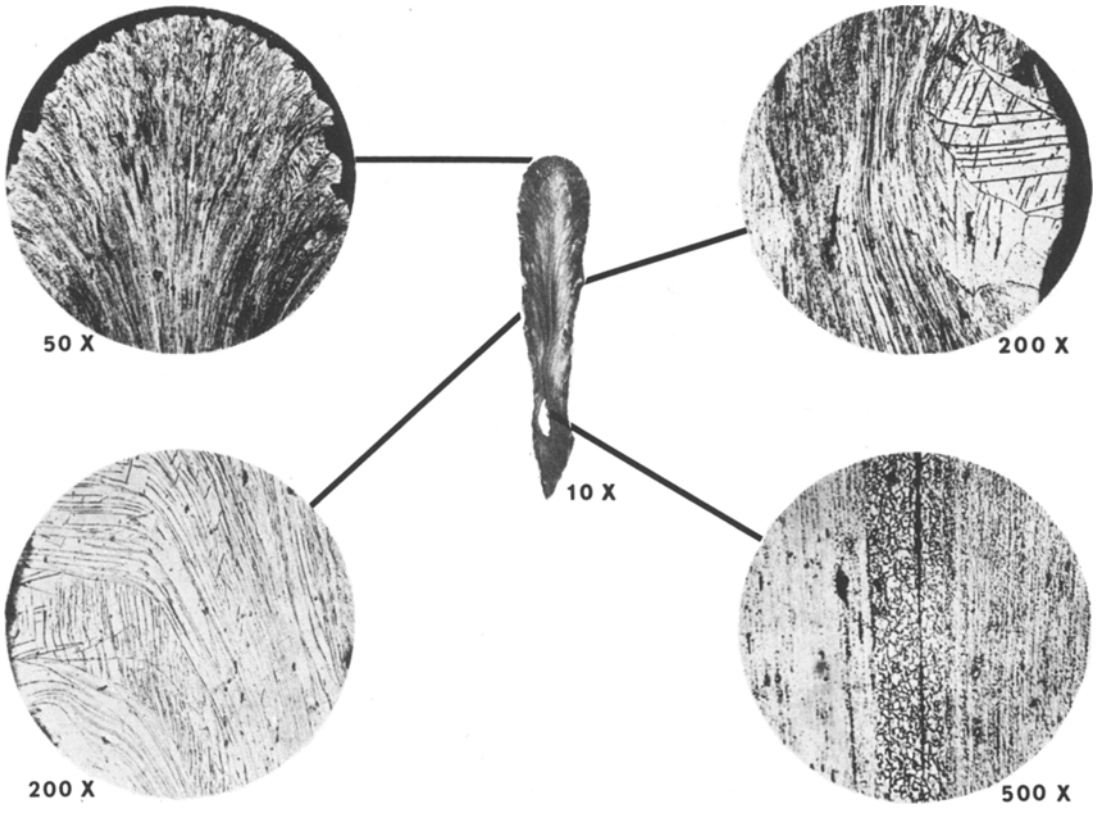

Figure 8 Cross-section and microstructure of jet formed from small, ductile liner.

trates the structure of the liner just as the jet is being formed. Note the jet being "squirted" forward, while at the same time the more massive slug is being generated. The similarity between the partially formed jet shown in Fig. 11 and the jet fragments illustrated earlier is also apparent.

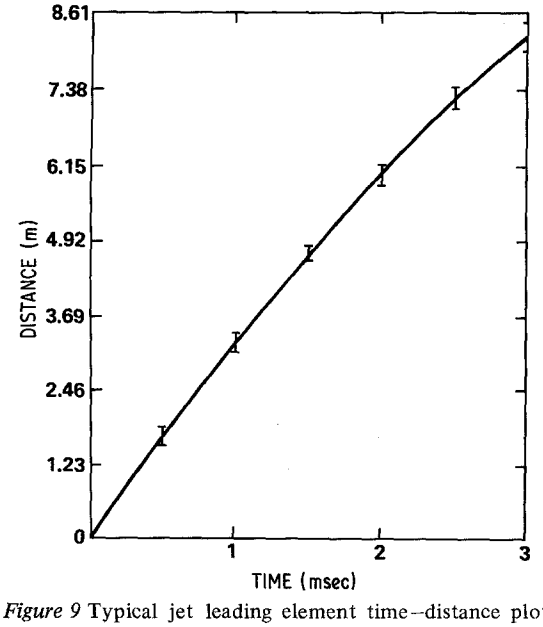

Figure 9 Typical jet leading element time–distance plot obtained from a timing screen array.

A model describing the sequential events leading up to liner collapse and jet/slug formation should explain the results of any of the tests described in this paper. A brief description of such a model is sequentially illustrated in Fig. 12.

Soon after being initiated at one end of the shaped-charge, the detonation shock wave reaches the apex of the liner, subjecting the outer surface to high pressure, causing the liner vanes to flow inward toward the liner apex. The pressure produced in the metal in the region where the vanes interact is probably of the order of 10^5 atm [5]. Material in this region behaves as an invisced fluid. The jet element begins to form forward, ahead of the converging vanes while the slug element forms behind. The inward-forward pressures cause the vanes to fracture from the remaining liner, and this tearing process causes the noticeable downward droop at the end of the wings shown in Figs. 7b and 12a.

Later, the explosive detonation progresses

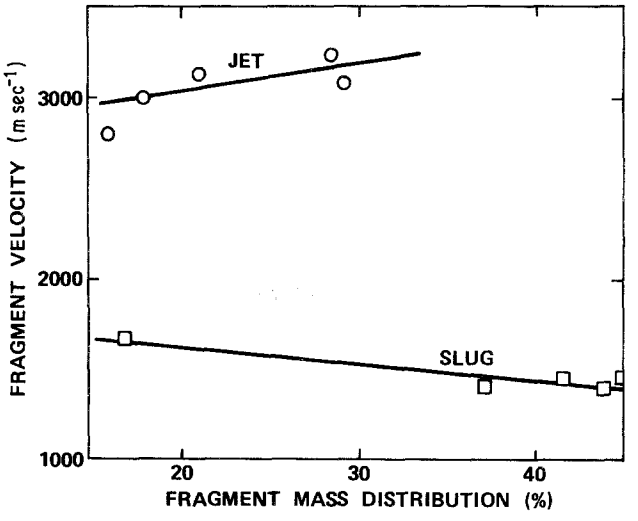

Figure 10 Relationship between jet/slug velocity and fragment weight distribution.

through the length of the device. The inward flow of metal continues, causing the wings to shorten, producing a single massive fragment. A velocity gradient exists within the fragment, resulting in elongation (Fig. 12b). When the elongation reaches a critical value in any region it results in the initiation of fracture.

Still later, the velocity gradient produces shear

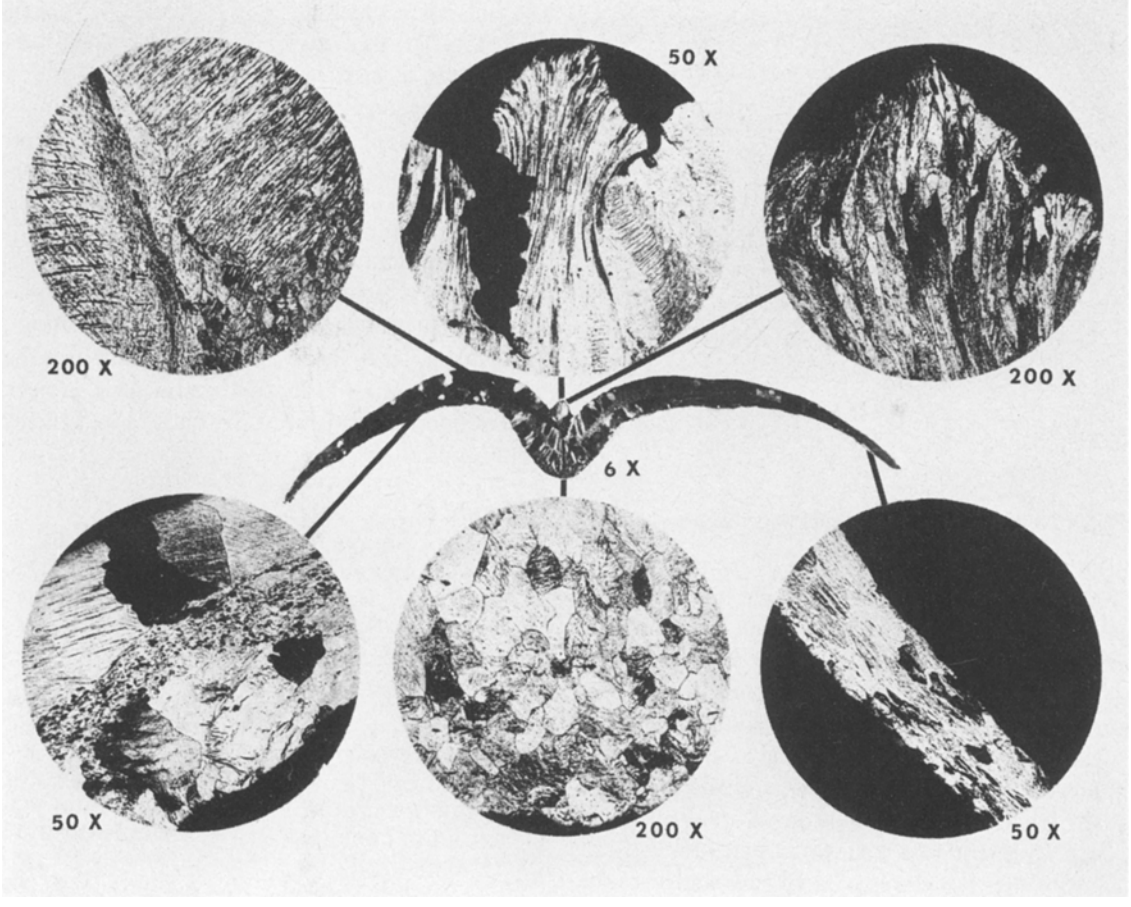

Figure 11 Cross-section and microstructure of partially collapsed liner.

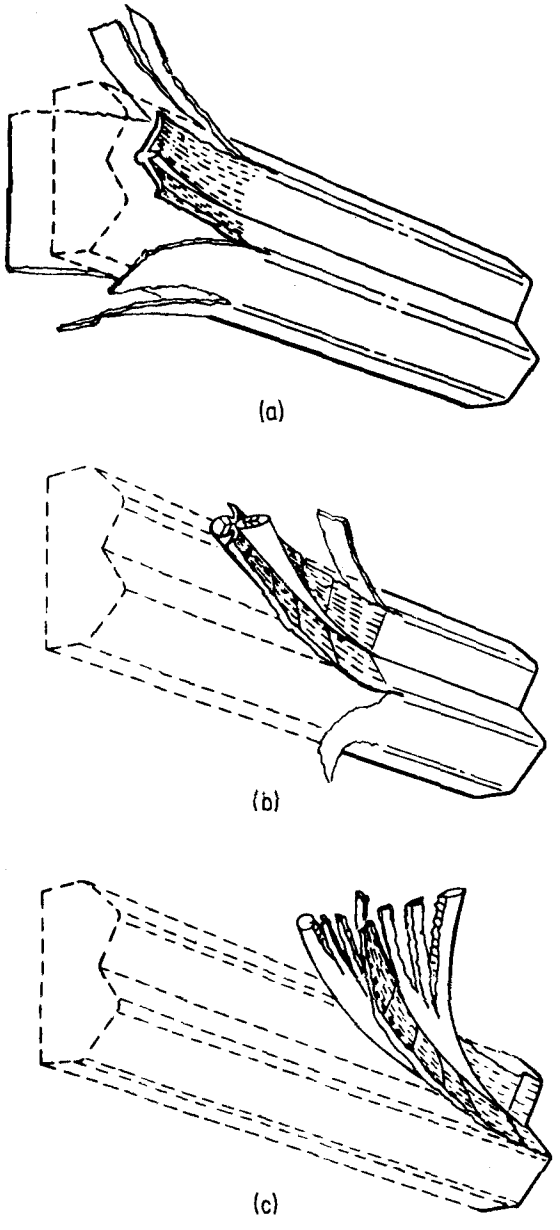

Figure 12 Illustration of proposed LSC collapse sequence.

fractures within the massive single fragment. The jet element fractures from the main fragment, and may in turn break into a leading jet and several slower jet followers. The slug element also fractures from the main fragment, and may in turn break into a massive slug and one or more jet wing followers. Separation of the jet and slug from the main fragment results in the remaining pair of jet wings. This sequence is shown in Fig. 12c.

Note that the pattern described is similar to the mock-ups shown previously in Fig. 3. The jet and slug are massive, rod-like fragments, and the jet wings have separated into two somewhat symmetrical fragments. The jet followers have broken up both longitudinally (in the recrystallized zone), and in the transverse direction. A velocity gradient exists between various elements of the shaped-charge. The jet travels at the highest velocity, with a progressive decrease in velocity of following elements down to the slug, which moves at the lowest velocity. It should be noted that the pattern described above for LSC fragment formation is in good agreement with that observed for conical-shaped-charge collapse [6].

5. Conclusions

1. Metallographic techniques provide a valuable tool for defining the deformation mechanisms involved in LSC fragment formation, and were used to postulate a model describing the sequence of events leading to LSC liner collapse.

2. Material properties and LSC liner geometry play an important role in determining the size, shape and velocity of LSC fragments, and influence the collapse mechanism.

3. The jet formed from a ductile LSC liner material is a massive, rod-like fragment. For a given LSC geometry, efficiency and jet velocity can be increased through the proper selection of materials possessing good ductility and high fracture toughness under high strain-rate conditions.

Acknowledgement

The author is grateful to Mr T. L. Herling who performed the metallography. Messrs R. A. Plauson, J. Whitson, and D. W. Lockwood supplied the test specimens used in this study. This project was supported by the US Naval Air Systems Command.

References

1. R. H. GOODENOW, *Trans. Q. ASM* 59 (1966) 804.
2. C. M. FOWLER, F. S. MINSHALL and E. G. ZUKAS, "Response of Metals to High Velocity Deformation" (Interscience, New York, 1961) p. 275.
3. H. F. KAISER and H. F. TAYLOR, *Trans. AIME* 27 (1939) 227.
4. Naval Weapons Center, "Warhead Department-Linear Shaped Charge Ejecta", China Lake, California, March 1968 (NWC TP 4100-9, Part 3).
5. G. BIRKHOFF, D. P. MACDOUGALL, E. M. PUGH and SIR G. TAYLOR, *J. Appl. Phys.* 19 (1948) 563.
6. R. S. EICHELBERGER and E. M. PUGH, *ibid.* 23 (1952) 537.

Received 24 November
and accepted 29 November 1983